ELSEVIER

Journal of Crystal Growth 230 (2001) 63–72

JOURNAL OF CRYSTAL GROWTH

www.elsevier.com/locate/jcrysgro

Effect of axial magnetic field on three-dimensional instability of natural convection in a vertical Bridgman growth configuration

A.Yu. Gelfgat*, P.Z. Bar-Yoseph, A. Solan

Faculty of Mechanical Engineering, Computational Mechanics Laboratory, Technion–Israel Institute of Technology, Haifa 32000, Israel

Abstract

A study of the effect of an externally imposed magnetic field on the axisymmetry-breaking instability of an axisymmetric convective flow, associated with crystal growth from bulk of melt, is presented. Convection in a vertical cylinder with a parabolic temperature profile on the sidewall is considered as a representative model. A parametric study of the dependence of the critical Grashof number Gr_{cr} on the Hartmann number Ha for fixed values of the Prandtl number ($Pr = 0.015$) and the aspect ratio of the cylinder ($A = \text{height/radius} = 1, 2$ and 3) is carried out. The stability diagram $Gr_{cr}(Ha)$ corresponding to the axisymmetric—three-dimensional transition for increasing values of the axial magnetic field is obtained. The calculations are done using the spectral Galerkin method allowing an effective and accurate three-dimensional stability analysis. It is shown that at relatively small values of Ha the axisymmetric flow tends to be oscillatory unstable. After the magnitude of the magnetic field (Ha) exceeds a certain value the instability switches to a steady bifurcation caused by the Rayleigh–Bénard mechanism.

PACS: 81.10; 47.20; 47.65

MSC: 65C20; 65M70

Keywords: A1. Computer simulation; A1. Convection; A1. Heat transfer; A1. Magnetic fields; A2. Bridgman technique

1. Introduction

The present study is focused on a particular problem of the electromagnetic control of convective melt flow [1] in Bridgman and related crystal growth technologies [2]. We study the possibility to stabilize an axisymmetric convective flow by an external axial magnetic field. Several previous studies considered mainly electromagnetic damping of the flow and its effect on the heat/mass transfer and dopant segregation [3–7]. Recent analysis of stability of steady state convective flows in a simplified Bridgman configuration [8] showed that, as a rule, the instability sets in with the breaking of axial symmetry of the flow. Therefore, analysis of stability and calculation of supercritical (steady or oscillatory) states should be done on the basis of three-dimensional models (see for example three-dimensional calculation in

*Corresponding author.
E-mail address: alexg@cmlp.technion.ac.il (A.Yu. Gelfgat).

0022-0248/01/$ - see front matter
PII: S0022-0248(01)01335-5

Ref. [9]). The effect of the magnetic field on the three-dimensional axisymmetry-breaking instability of initially axisymmetric steady convective flows was studied recently in Refs. [10,11]. The temperature boundary conditions considered in these studies corresponded to the Rayleigh–Bénard configuration, i.e. isothermal top and bottom and thermally insulated side boundary of a vertical cylinder. Electromagnetic stabilization of axisymmetric convective flows for more complicated thermal conditions was not studied.

In the present paper, we continue our previous study [8] and consider the effect of an axial magnetic field on the axisymmetry-breaking instability of convective flow in a vertical cylinder with parabolic temperature profile on the sidewall. The parabolic temperature profile is taken as an example of arbitrary heating/cooling conditions which have to be imposed in specific practical cases. A parametric study of stability of the flow for increasing values of magnetic field strength (the Hartmann number Ha) is performed for a fixed value of the Prandtl number ($\mathrm{Pr}=0.015$) and three fixed values of the aspect ratio ($A=$height/radius) of the cylinder, equal to 1, 2 and 3. The corresponding stability diagram, showing the dependence of the critical Grashof number ($\mathrm{Gr}_{\mathrm{cr}}$) on Ha, is presented. It is shown that for the axial magnetic field the electromagnetic stabilization is stronger in lower cylinders. It is found also that after the magnetic field exceeds a certain value the type of instability changes, such that the oscillatory instability of the flow (Hopf bifurcation) is replaced by a bifurcation from steady axisymmetric to steady asymmetric flow state. The patterns of flows and the most dangerous perturbations presented allow us to derive some additional conclusions about the nature of the instability observed.

2. Formulation of the problem and numerical technique

We consider convection of an incompressible Boussinesq fluid in a vertical cylindrical container of radius R and height H, subject to a constant external vertical and homogeneous magnetic field $\boldsymbol{B}=\{0,\,0,\,B_0\}$. Interaction of the magnetic field with the convective flow induces the electric current

$$\mathbf{j}=\sigma[-\nabla\phi+\mathbf{v}\times\mathbf{B}], \tag{1}$$

where $\mathbf{v}=\{v_r,\,v_\varphi,\,v_z\}$ is velocity, ϕ is electric potential and σ is electric conductivity of the fluid. Conservation of the induced electric current, $\nabla\cdot\mathbf{j}=0$, yields the equation for the electric potential

$$\Delta\phi=B_0\mathbf{e}_z\cdot\nabla\times\mathbf{v}=-\frac{B_0}{r}\left[\frac{\partial v_r}{\partial\varphi}-\frac{\partial(rv_\varphi)}{\partial r}\right]. \tag{2}$$

The flow is described by the dimensionless three-dimensional Navier–Stokes, continuity and energy equations

$$\begin{aligned}\frac{\partial\mathbf{v}}{\partial t}+(\mathbf{v}\cdot\nabla)\mathbf{v}=&-\nabla p+\Delta\mathbf{v}+\mathrm{Gr}T\mathbf{e}_z\\&-\mathrm{Ha}^2\left[-\frac{\partial\phi}{\partial r}\mathbf{e}_\varphi+\frac{1}{r}\frac{\partial\phi}{\partial\varphi}\mathbf{e}_r\right.\\&\left.+v_r\mathbf{e}_r+v_\varphi\mathbf{e}_\varphi\right],\end{aligned} \tag{3}$$

$$\nabla\cdot\mathbf{v}=0, \tag{4}$$

$$\frac{\partial T}{\partial t}+(\mathbf{v}\cdot\nabla)T=\frac{1}{\mathrm{Pr}}\Delta T \tag{5}$$

in the domain $0\leqslant r\leqslant 1$, $0\leqslant z\leqslant A$, $0\leqslant\varphi\leqslant 2\pi$. Here $\mathbf{v}$, T, p, and $\mathbf{B}$ are non-dimensional velocity, temperature, pressure, and magnetic field, respectively. The dimensional scales of the time, the velocity and the pressure are R^2/ν, ν/R and $\rho(\nu/R)^2$, respectively. The temperature is non-dimensionalized as $T=(T^*-T_{\mathrm{melt}})/(T_{\max}-T_{\mathrm{melt}})$. The magnetic field is scaled by B_0. Other parameters are: $\mathrm{Gr}=g\beta\Delta TH^3/\nu^2$ Grashof number, $\mathrm{Pr}=\nu/\chi$ Prandtl number, $\mathrm{Ha}=B_0l\sqrt{\sigma/\rho\nu}$ Hartmann number, g gravity acceleration in the z-direction, β thermal expansion coefficient, ν viscosity; χ heat diffusivity, and ρ density. T^* is the dimensional temperature, $T_{\max}$ is the maximal temperature at the sidewall and T_{melt} is the melting temperature imposed at the top and the bottom.

Similarly to our previous study [8], we consider no-slip boundary conditions for velocity, a *parabolic* temperature profile at the sidewall of the cylinder and equal constant temperatures at the

top and bottom. Additionally, we assume that all the boundaries are electric insulators. These read

$$\text{at } z = 0 \text{ and } A: \quad T = 0, \quad \mathbf{v} = 0, \quad \frac{\partial \phi}{\partial z} = 0, \quad (6)$$

$$\text{at } r = 1: \quad T = z(1 - z/A), \quad \mathbf{v} = 0, \quad \frac{\partial \phi}{\partial r} = 0. \quad (7)$$

The boundary conditions at the axis should be added for the axisymmetric basic state flow

$$\text{at } r = 0: \quad \frac{\partial T}{\partial r} = 0, \quad v_r = 0,$$

$$v_\varphi = 0, \quad \frac{\partial v_z}{\partial r} = 0, \quad \frac{\partial \phi}{\partial r} = 0. \quad (8)$$

These boundary conditions allow the existence of an axisymmetric steady solution of Eqs. (1)–(8). As it is noticed in Ref. [8], the shape of the temperature profile at the sidewall is arbitrary and can be replaced by a more complicated boundary condition.

The effect of the induced electric currents on the external magnetic field and the Joule heating are neglected in the formulation (1)–(8). This is justified by the estimation of non-dimensional parameters characteristic for liquid metals and semiconductors (some details are given in Ref. [12]).

The numerical technique applied is the same as was used in Ref. [8]. The 2π-periodicity of the solution of Eqs. (2)–(8) allows its representation as a Fourier series

$$\{\mathbf{v}, p, T, \phi\} = \sum_{k=-\infty}^{k=\infty} \{\mathbf{v}_k, p_k, T_k, \phi_k\} \exp(\mathrm{i}k\varphi). \quad (9)$$

Then, we are looking for values of Gr number for which the steady axisymmetric solution $\{\mathbf{v}_0(r,z), p_0(r,z), T_0(r,z), \phi_0(r,z)\}$ becomes unstable with respect to the axisymmetric ($k = 0$) or non-axisymmetric ($k \neq 0$) perturbations. The linear stability problem separates for each value of the azimuthal wavenumber k [13]. Therefore, for each k one has to consider a quasi-axisymmetric problem that yields the critical Grashof number $\mathrm{Gr}_{\mathrm{cr}}(\mathrm{Ha}, \mathrm{Pr}, A, k)$. Finally, the critical Grashof number is defined as $\mathrm{Gr}_{\mathrm{cr}}(\mathrm{Ha}, \mathrm{Pr}, \mathrm{A}) = \min_k \mathrm{Gr}_{\mathrm{cr}}(\mathrm{Ha}, \mathrm{Pr}, A, k)$, and the value $k = k_{\mathrm{cr}}$ which yields the minimum of $\mathrm{Gr}_{\mathrm{cr}}(\mathrm{Ha}, \mathrm{Pr}, A, k)$ is the critical wavenumber. In the case of oscillatory instability the critical frequency of oscillations ω_{cr} (the oscillation frequency at $\mathrm{Gr} = \mathrm{Gr}_{\mathrm{cr}}$) should be added to the set of critical parameters. The dimensional scale for ω_{cr} is v/R^2. The calculations were carried out using the global Galerkin method described in Ref. [13]. To ensure the correctness of results an additional convergence study was performed for $\mathrm{Pr} = 0.015$ and Ha varying from 0 to 100. Similarly to the results of Ref. [8], it showed that truncation of the Galerkin series to 30×30 basis functions in the r- and z-directions yields 3–4 correct digits in the critical $\mathrm{Gr}_{\mathrm{cr}}$ and the critical frequency. It was found also that the instability sets in before the Hartmann boundary layers develop. For that reason the slowdown of the numerical convergence for increasing Ha, reported in [12], was not observed.

3. Results

The calculations were performed for a fixed value of the Prandtl number, $\mathrm{Pr} = 0.015$, and three fixed values of the aspect ratio $A = 1$, 2 and 3. For each value of the aspect ratio a family of curves $\mathrm{Gr}_{\mathrm{cr}}(\mathrm{Ha}, k)$ was calculated for k varying from 0 to 20. Examples for three fixed pairs of Ha and A are shown in Table 1. The final marginal stability curve was obtained as the lower envelope of all curves $\mathrm{Gr}_{\mathrm{cr}}(\mathrm{Ha}, k)$ (for details see Ref. [8]). The final result is shown in Fig. 1 as a dependence of $\mathrm{Gr}_{\mathrm{cr}}$ on Ha for different aspect ratios. The critical azimuthal wavenumbers are indicated on each continuous branch of the curves.

The stabilization of convective flow by the external magnetic field, i.e., the growth of $\mathrm{Gr}_{\mathrm{cr}}$ with the increase of Ha, is clearly seen in Fig. 1. The growth is monotonic except a short interval $20.5 < \mathrm{Ha} < 22$ at $A = 3$, where a tiny decrease of the $\mathrm{Gr}_{\mathrm{cr}}$ number is connected with the switch of the dominant perturbation mode (see below). At the same time, one can see that in lower cavities ($A = 1$) the stabilization is considerably stronger than in taller ones ($A = 3$). We explain this by the interaction of the vertically directed magnetic field with the convective roll. The electromagnetic force in Eq. (3) is generated by the interaction of the

magnetic field with radial and azimuthal component of the velocity (the latter appears only as a part of three-dimensional perturbation), but not with the axial velocity. The axial velocity is affected only via continuity. Therefore, in taller cylinders, where the axial velocity of the convective roll is larger than the radial and the azimuthal ones (see flow patterns described below) the electromagnetic suppression of the base flow is weaker. Consequently, stronger magnetic field is required to reach a certain stabilization. Thus, to increase the Gr_{cr} to 5×10^6 one needs Ha $\approx$ 25 for $A=1$, Ha $\approx$ 41 for $A=2$, and Ha $\approx$ 58 for $A=3$. We expect an opposite trend for a transverse magnetic field.

Table 1
Critical Grashof numbers ($Gr_{cr}\times10^{-6}$) for different azimuthal number k. Values, close to the critical one, are shown in bold

k	$A=1$, Ha = 20	$A=2$, Ha = 40	$A=3$, Ha = 60
0	13.627	6.865	6.561
1	6.030	23.974	14.331
2	13.013	5.728	**5.410**
3	9.211	6.282	6.700
4	6.369	5.582	6.167
5	4.726	5.112	5.737
6	3.946	**4.885**	**5.509**
7	3.586	**4.830**	**5.447**
8	3.374	**4.898**	**5.516**
9	**3.266**	5.063	5.698
10	**3.237**	5.317	5.988
11	**3.269**	5.661	6.406
12	3.351	6.107	7.070
13	3.476	6.682	7.856
14	3.641	7.428	9.148
15	3.848	8.423	10.538
16	4.095	9.750	11.617
17	4.328	11.215	12.655
18	4.712	12.492	13.895
19	5.085	13.693	15.547
20	5.503	14.999	17.756

For all values of the aspect ratio considered the instability sets in as a Hopf bifurcation (oscillatory instability) at low values of Ha, while at larger Ha the instability appears as a transition from steady axisymmetric to steady non-axisymmetric flow. The switch from Hopf to steady bifurcation takes place at Ha $\approx$ 10 at $A=1$, Ha $\approx$ 31 at $A=2$, and Ha $\approx$ 20.5 at $A=3$. The circular frequencies of the oscillations (defined as imaginary part of the dominant eigenvalue [13]) for Hartmann numbers corresponding to the Hopf bifurcation are shown in Fig. 2.

Another effect of the increasing magnetic field is the growth of the critical azimuthal wavenumber k_{cr}, which is seen in Fig. 1 for $A=1$ starting from Ha = 12.5, and 2 starting from Ha $\approx$ 32. For $A=3$

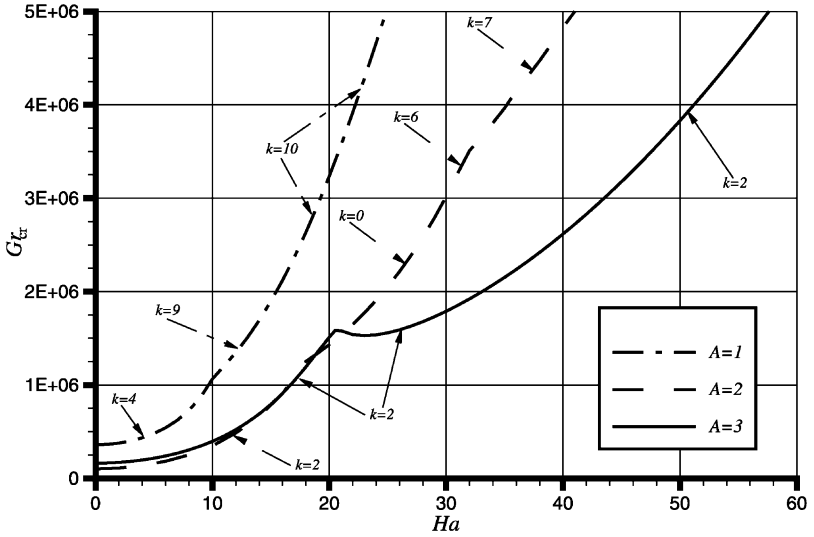

Fig. 1. Critical Grashof number versus Hartmann number.

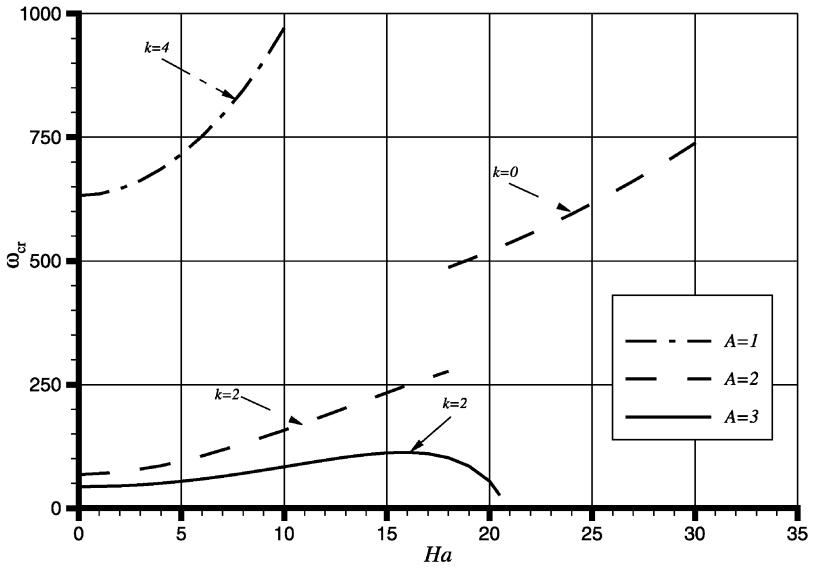

Fig. 2. Circular frequency of oscillations at the critical value of Gr versus Hartmann number.

the growth of k_{cr} takes place for values of Ha larger than 60. An important property of the instability at relatively large Hartmann numbers is the existence of several perturbation modes with different azimuthal wavenumbers k, but with Grashof numbers very close to the critical one. This is illustrated in Table 1, where the values of Gr_{cr}, which are less than 2% different from $\min_k Gr_{cr}(Ha, Pr, A, k)$, are shown in bold. This means that already at small supercriticalities one can expect multiplicity of supercritical states, such that the final asymptotic state is defined not only by the governing parameters, but also by the initial conditions. Another possibility is the non-linear interaction between different modes, which can lead to very complicated patterns of supercritical flows.

A better understanding of the mechanisms that cause the switch from Hopf to steady bifurcation and the growth of the azimuthal wavenumber, can be drawn from the patterns of the flow and the most dangerous perturbation. The latter grows exponentially after the instability sets in. Figs. 3–9 illustrate streamlines and isotherms of the axisymmetric flow at critical parameters together with patterns of the most dangerous perturbations. All isolines and isosurfaces in Figs. 3–9 are equally distanced. The maximal values of stream function are shown in each figure. The dimensionless temperature varies between 0 and 1. The perturbations (which are the eigenvectors of linear stability problem) are defined to within multiplication by a constant and therefore, their numerical values are arbitrary.

The physical meaning of the perturbation patterns differs for different bifurcation types. Thus, for an axisymmetric Hopf bifurcation (observed for $A=2$, $18<Ha<31$) we plot the modulus of perturbation, which coincides, to within multiplication by a constant, with the amplitude of oscillations of the supercritical flow. In the case of an axisymmetry-breaking Hopf bifurcation the isosurfaces of perturbation describe (also to within multiplication by a constant) the amplitude of a traveling wave propagating in the azimuthal direction with the group angular velocity ω_{cr}/k (see Ref. [13] for details). In the case of a steady axisymmetry-breaking bifurcation the perturbation depicts a pattern of the supercritical flow itself, rather than its deviation from the unstable axisymmetric state (see, for example, Ref. [14]).

An example of the flow and perturbation patterns corresponding to the axisymmetric Hopf bifurcation is shown in Fig. 3. It is seen that the

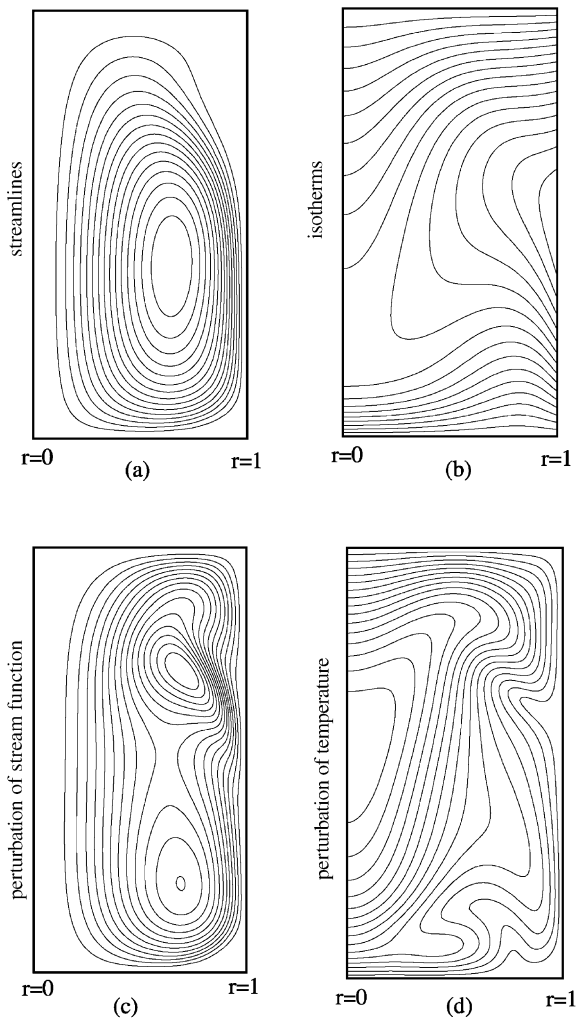

Fig. 3. Patterns of the flow and the most dangerous perturbation for the *axisymmetric* Hopf bifurcation. $A=2$, $\mathrm{Pr}=0.015$, $\mathrm{Ha}=30$, $\mathrm{Gr_{cr}}=3.02\times10^6$: (a) streamlines, $|\psi|_{\max}=132.83$; (b) isotherms; (c) amplitude of the most dangerous perturbation of the stream function; (d) amplitude of the most dangerous perturbation of the temperature.

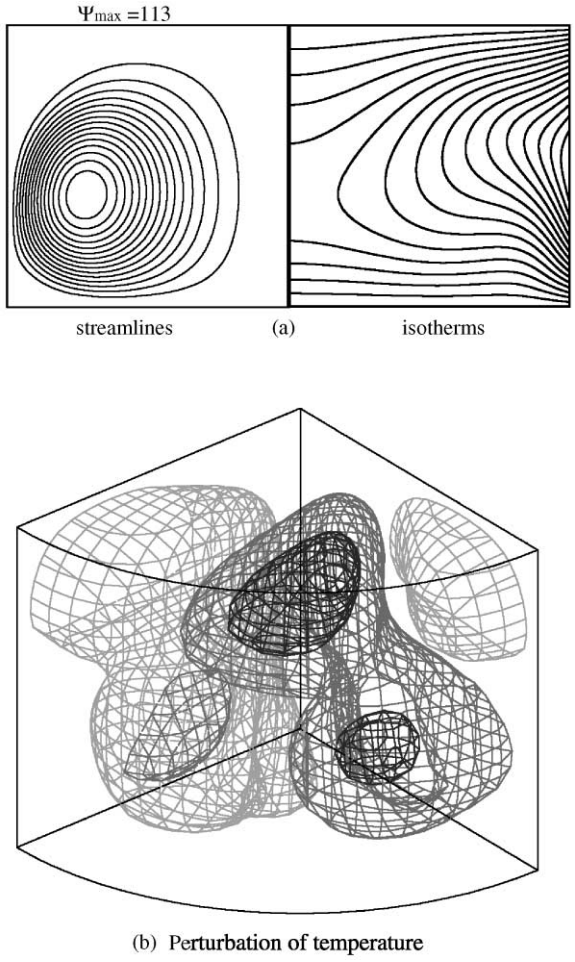

Fig. 4. Patterns of the flow and the most dangerous perturbation of the temperature for the *axisymmetry-breaking* Hopf bifurcation. $A=1$, $\mathrm{Pr}=0.015$, $\mathrm{Ha}=10$, $k_{\mathrm{cr}}=4$, $\mathrm{Gr_{cr}}=1.06\times10^6$: (a) streamlines and isotherms of the axisymmetric base state; (b) isosurfaces of the temperature perturbations.

perturbation (amplitude of oscillations) is spread over all the bulk of the flow with the maximum of temperature pulsations on the axis. Such a bulk distribution of the perturbation is characteristic also for the axisymmetry-breaking Hopf bifurcation. The corresponding illustrations are given in Figs. 4 and 5. To illustrate the three-dimensionality of the perturbation better, we also show the isolines of the temperature perturbation in the cross section $z=3A/4$ (Fig. 6). The patterns shown in Fig. 6 rotate with the angular velocity $\omega_{\mathrm{cr}}/k_{\mathrm{cr}}$. The direction of rotation is arbitrary because the azimuthal velocity of the base flow is zero.

Note, that the perturbation of the temperature in Fig. 5b has a global maximum and minimum in the upper part of the cylinder where the isotherms of the base flow (Fig. 5a) form an unstably stratified layer. This unstable stratification

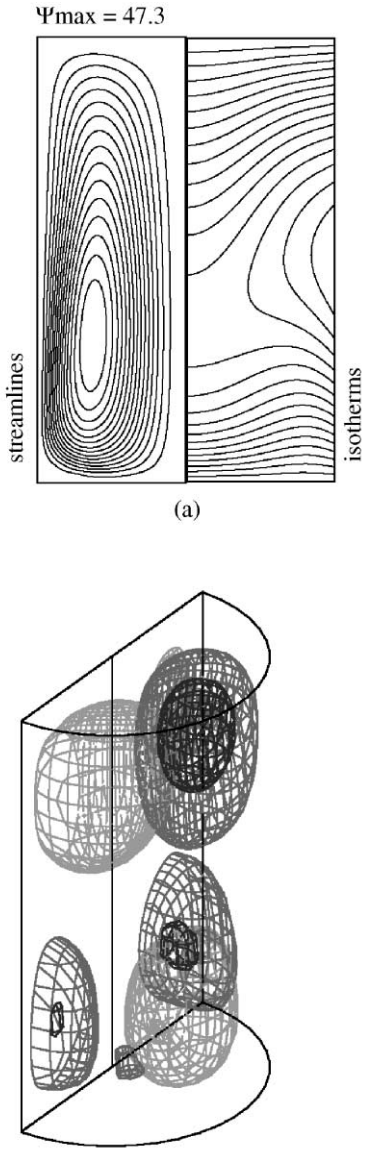

Fig. 5. As Fig. 4. $A=3$, $\mathrm{Pr}=0.015$, $\mathrm{Ha}=10$, $k_{cr}=2$, $\mathrm{Gr}_{cr}=3.96\times10^5$.

switches on the Rayleigh-Bénard instability mechanism, which usually leads to a steady bifurcation. The effect of the Rayleigh–Bénard mechanism is seen in the dependence $\omega_{cr}(\mathrm{Ha})$ for $A=3$ (Fig. 2), where the critical frequency rapidly decreases to zero in the interval $20<\mathrm{Ha}<21$.

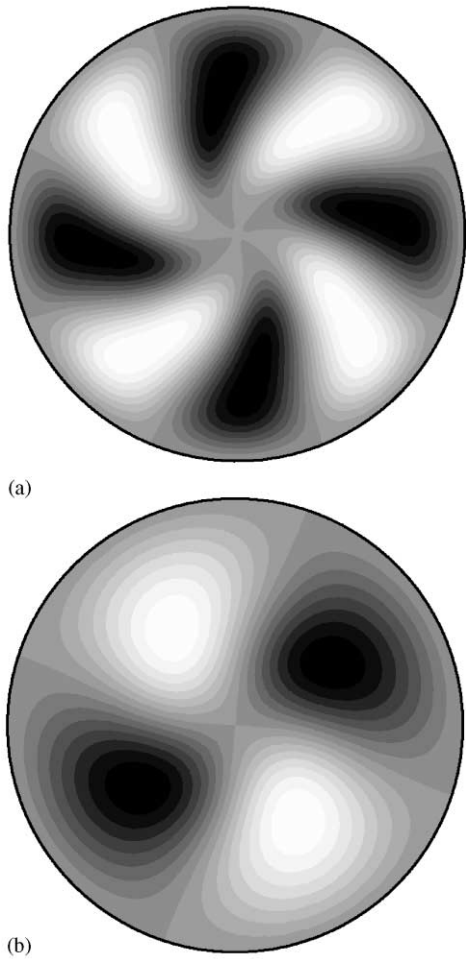

Fig. 6. Isolines of the temperature perturbation at the cross-section $z=3A/4$ for the *axisymmetry-breaking* Hopf bifurcation. (a) $A=1$, $\mathrm{Pr}=0.015$, $\mathrm{Ha}=10$, $k_{cr}=4$, $\mathrm{Gr}_{cr}=1.06\times10^6$; (b) $A=3$, $\mathrm{Pr}=0.015$, $\mathrm{Ha}=10$, $k_{cr}=2$, $\mathrm{Gr}_{cr}=3.96\times10^5$.

It was already shown in Ref. [8] that in tall cylinders in the absence of the magnetic field the Rayleigh–Bénard mechanism is responsible for the axisymmetry-breaking instability. A similar mechanism was observed in a short cylinder in Ref. [14], where an unstably stratified thermal layer developed. Under the electromagnetic effect considered here this mechanism becomes dominant at relatively large Ha even in short cylinders and results in a steady symmetry-breaking bifurcation. This is illustrated in Figs. 7 and 8.

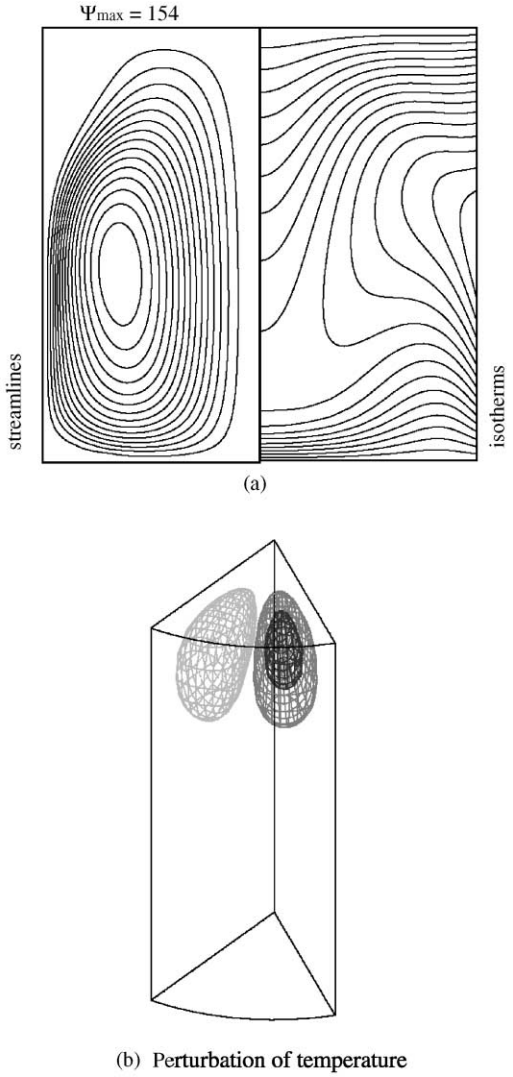

Fig. 7. Patterns of the flow and the most dangerous perturbation of the temperature for the *axisymmetry-breaking* steady bifurcation $A=2$, $\mathrm{Pr}=0.015$, $\mathrm{Ha}=40$, $k_{cr}=7$, $\mathrm{Gr}_{cr}=4.83\times10^6$: (a) streamlines and isotherms of the axisymmetric base state; (b) isosurfaces of the temperature perturbations.

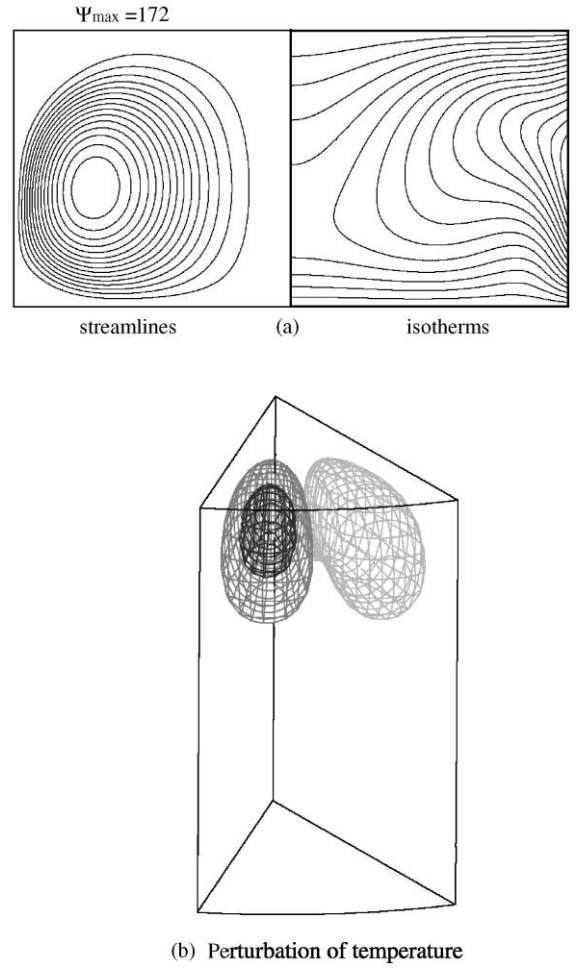

Fig. 8. As Fig. 7. $A=1$, $\mathrm{Pr}=0.015$, $\mathrm{Ha}=20$, $k_{cr}=10$, $\mathrm{Gr}_{cr}=3.24\times10^6$.

Fig. 7 shows the flow and perturbation patterns in the case $A=2$ and $\mathrm{Ha}=40$. The perturbations patterns can be interpreted as two convective rolls located in the upper part of the cylinder where the fluid is unstably stratified. The motion along these rolls takes place mainly in φ–z planes. This type of instability becomes dominant when the magnetic field exceeds a certain value such that the previously observed oscillatory instability is damped. A similar situation takes place also in lower cylinders, which is illustrated in Fig. 8 for $A=1$. For better illustration of the azimuthal structure of perturbations the isolines of temperature perturbation in the cross section $z=0.95\,A$ (just below the upper boundary) are shown in Fig. 9. Note that in these cases (steady bifurcation) all the patterns are stationary. The perturbation patterns shown in Figs.7–9 are similar to those observed in Ref. [14] for another problem of convection in a circular cylinder. As was noticed in

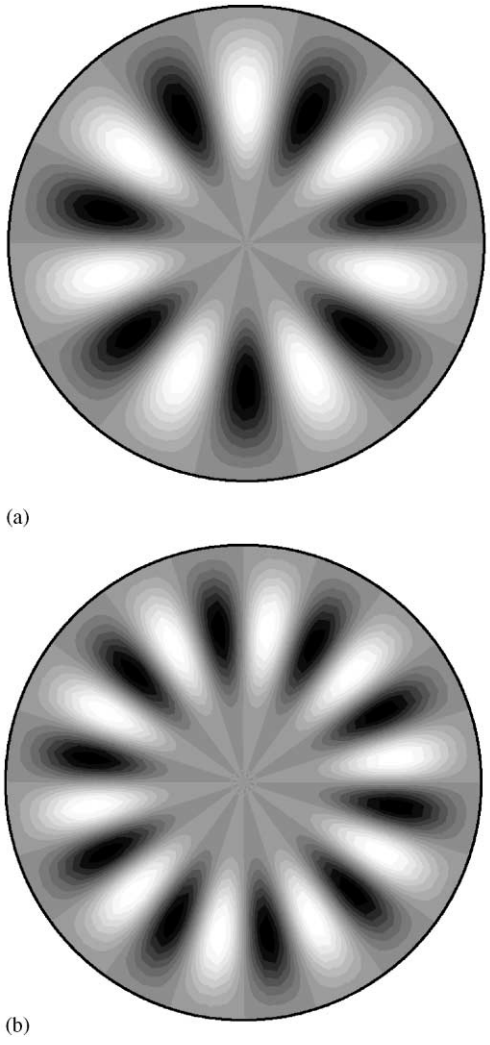

Fig. 9. Isolines of the temperature perturbation at the cross section $z=0.95$ for the *axisymmetry-breaking* steady bifurcation (a) $A=2$, $\mathrm{Pr}=0.015$, $\mathrm{Ha}=40$, $k_{cr}=7$, $\mathrm{Gr}_{cr}=4.83\times10^6$; (b) $A=1$, $\mathrm{Pr}=0.015$, $\mathrm{Ha}=20$, $k_{cr}=10$, $\mathrm{Gr}_{cr}=3.24\times10^6$.

Ref. [8] these structures seem to be rather common and can be expected whenever an unstably stratified thermal layer develops in the bulk of the flow. The rolls developing due to the Rayleigh–Bénard instability have almost square cross section, such that their size is defined by the depth of the unstably stratified layer. Smaller rolls develop in thinner layers and consequently have larger critical azimuthal wavenumber k_{cr} [14]. In the problem considered here we observe a certain decrease of the depth of the unstably stratified layer with the increase of the Hartmann number for $A=1$ and 2. Together with that, at large Hartmann numbers we observe a growth of k_{cr} with the increasing Ha (Fig. 1).

4. Concluding remarks

As was stated in Ref. [8], the simplified model presented here should be considered as an illustration of the effect of electromagnetic stabilization of an axisymmetric flow. Our experience shows (see Refs. [8,12–14] and references therein) that the dependence of stability properties on geometry, boundary conditions and governing parameters can be very strong, such that no extrapolation of quantitative results to other problems is possible. However, some general qualitative conclusions on the effect of axial magnetic field on the stability of axisymmetric convective flows can be drawn from the results presented.

It was shown that the electromagnetic stabilization is weaker for taller cylinders, which is explained by the elongation of the convective roll along the magnetic field and consequent weaker electromagnetic damping. A similar effect was observed also for rectangular configurations [12]. A rather unexpected result is the replacement of the oscillatory instability by steady bifurcations, which was observed for relatively large Hartmann numbers and is caused by the Rayleigh–Bénard instability mechanism. This effect can lead to a situation where no thermal oscillations are observed, but the distribution of dopants (or impurities) is azimuthally non-uniform due to a steady three-dimensional flow pattern. It was found also that the critical azimuthal wavenumber, corresponding to these bifurcations, grows with the increase of magnetic field, which can lead to stronger azimuthal inhomogeneities under stronger electromagnetic effect.

Acknowledgements

This work was supported by the Israel Ministry of Science (Grant 8575-1-98), the Israel Ministry

of Immigrant Absorption (to A. Gelfgat), the Israel High Performance Computer Unit, the Fund for Promotion of Research and the Y. Winograd Chair of Fluid Dynamics and Heat Transfer at Technion.

References

[1] J.S. Walker, Models of melt motion, heat transfer and mass transport during crystal growth with strong magnetic fields, Progr. Cryst. Growth Charact. Mater. 38 (1999) 195.
[2] J.P. Garandet, T. Alboussierre, Bridgman growth: modeling and experiments, Progr. Cryst. Growth Charact. Mater. 38 (1999) 73.
[3] G.M. Oreper, J. Szekely, The effect of a magnetic field on transport phenomena in a Bridgman–Stockbager crystal growth, J. Crystal Growth 67 (1984) 405.
[4] D.H. Kim, P.M. Adornato, R.A. Brown, Effect of vertical magnetic field on convection and segregation in vertical Bridgman crystal growth, J. Crystal Growth 89 (1988) 339.
[5] D.A. Watring, S.L. Lehoczky, Magneto-hydrodynamic damping of convection during vertical Bridgman–Stockbarger growth of HgCdTe, J. Crystal Growth 167 (1996) 478.
[6] M. Yao, A. Chait, A.L. Fripp, W.J. Debnam, Magnetically damped convection and segregation in Bridgman growth of PbSnTe, J. Crystal Growth 173 (1997) 467.
[7] N. Ma, J.S. Walker, A parametric study of segregation effects during vertical Bridgman crystal growth with an axial magnetic field, J. Crystal Growth 208 (2000) 757.
[8] A.Yu. Gelfgat, P.Z. Bar-Yoseph, A. Solan, Axisymmetry-breaking instabilties of natural convection in a vertical Bridgman growth configuration, J. Crystal Growth 220 (2000) 316.
[9] C.J. Jing, N. Imaishi, S. Yasuhiro, T. Sato, Y. Miyazawa, Three-dimensional numerical simulation of rotating spoke pattern in an oxide melt under a magnetic field, Int. J. Heat Mass Transfer 43 (2000) 4347.
[10] R. Touihri, H. Ben Hadid, D. Henry, On the onset of convective instabilities in cylindrical cavities heated from below, Phys. Fluids 11 (1999) 2089.
[11] M. Prange, M. Wanschura, H.C. Kuhlmann, H.J. Rath, Linear stability of thermocapillary convection in cylindrical liquid bridges under axial magnetic fields, J. Fluid Mech. 394 (1999) 281.
[12] A.Yu. Gelfgat, P.Z. Bar-Yoseph, On the magnetic field effect on oscillatory instability of convective flows in a rectangular cavity, Phys. Fluids, submitted for publication.
[13] A.Yu. Gelfgat, Two- and three-dimensional instabilities of confined flows: numerical study by a global Galerkin method, Comput. Fluid Dyn. J. 9 (2000) 1.
[14] A.Yu. Gelfgat, P.Z. Bar-Yoseph, A. Solan, T. Kowalewski, Axisymmetry-breaking bifurcations in axially symmetric natural convection, Int. J. Transport Phenom. 1 (1999) 173.